Photoelectron Holography

John J. Barton
IBM T. J. Watson Research Center, Yorktown Heights, New York 10498
(Received 6 July 1988)

A photoelectron hologram is a two-angle photoelectron diffraction pattern: Direct photoemission plays the role of the reference wave and the scattered waves are the object waves. When the hologram is created from the core-level photoemission of single emitting species on an ordered surface, a complete three-dimensional image of the surface structure surrounding the emitter can be reconstructed by Fourier transformation.

PACS numbers: 42.40.Dp, 61.14.Dc

Recently, Szöke[1] suggested that electron microscopy could be done with photoelectrons, by measuring and reconstructing a photoelectron hologram. In this Letter, I show that this idea can be restated as follows: The phenomenon we know as photoelectron diffraction[2] can be interpreted as photoelectron holography. A two-dimensional photoelectron diffraction pattern is a hologram which can be reconstructed to create an "image" of the three-dimensional crystal structure of a solid surface.

Photoelectron diffraction occurs when a photoemitted electron finds more than one path into a photoelectron detector. One path is provided by direct propagation to the detector, while additional paths are available when the photoelectron scatters elastically from nearby atoms. In the time since Liebsch[2] first suggested that photoelectron diffraction could be observed from adsorbates on surfaces and that the interference pattern would contain information about the geometry of atoms surrounding the photoemitting adsorbate, many experimental measurements have been made, both confirming the phenomenon and using it to determine surface structure. The structure information is extracted primarily by trial-and-error fits of scattering simulations to diffraction measurements.[3-5] Semiquantitative geometry information has been obtained by direct Fourier analysis of the energy-dependent diffraction measurements[3,6] and, in favorable cases, lobes in angular scans can be attributed to particular strong scattering events giving clues to structure.[5,7]

Apparently unaware of the photoelectron diffraction work, Szöke proposed that electron holography could be done with photoelectrons or Auger decay electrons. A hologram is created when a reference wave interferes with object waves to create a diffraction pattern. The connection between holography and photoelectron diffraction is most easily made by considering the holography geometry proposed in Gabor's original papers introducing holography.[8,9] Gabor proposed using a point source of monochromatic electrons illuminating a semitransparent object and recording the transmitted signal. In photoelectron holography, the source of monochromatic spherical waves is the photoemission final state. To insure a point source we restrict our attention to core-level photoemission. The objects are nearby ion cores which scatter the photoelectron: The source-to-object distances are of atomic dimensions and the objects may be behind, in front of, or beside the source. The wavelength of the radiation is given by the de Broglie relation, e.g., electrons of 400 eV will have wavelengths of 0.6 Å. Each photoemission event yields only one photoelectron so a great many identical source-object arrangements must be averaged to generate the hologram.

With this identification we can state that the reported work on photoelectron diffraction is experimental proof that Szöke's photoelectron holograms are measurable, and we are led to immediately attempt to image a surface structure by "wave-front reconstruction" of a photoelectron diffraction hologram. This Letter demonstrates a practical method of imaging photoelectron holograms by reconstructing an image of a surface structure from a simulated hologram.

The physics of photoelectron diffraction is sufficiently well understood and tested experimentally[10] that we may confidently simulate a photoelectron hologram by numerical calculation. We define a normalized hologram function $\chi(\hat{\mathbf{K}})$ by removing the reference wave as much as possible:

$$\chi(\hat{\mathbf{K}}) = (I - I_0)/\sqrt{I_0}$$
$$= \sum_j |F_j(\theta_{r_jK})| \cos[kr_j - \mathbf{r}_j \cdot \hat{\mathbf{K}} + \phi_j(\theta_{r_jK})], \quad (1)$$

where $I_0 = \psi_0^* \psi_0$ is the reference intensity, $F_j = |F_j| \times \exp(i\phi_j)$ is a generalized scattering factor, $\hat{\mathbf{K}}$ is the emission vector, and r_j is the total length of the path from the emitter to the end of the jth scattering path. The vector $\mathbf{r}_j$ runs from the emitter to the last scattering atom on the jth path. The generalized scattering factor F_j includes elastic- and inelastic-scattering factors as well as wave-front curvature corrections[11]; the sum on j is extended to all multiple-scattering events with significant amplitude.

The hologram function $\chi(\hat{\mathbf{K}})$ contains just the oscillat-

ing (interference) part of the hologram. To create an image from this hologram, we imagine printing $\chi(\hat{\mathbf{K}})$ onto a film and irradiating it with a converging spherical wave. Of course, such a process may not be practical, but we may nevertheless compute the image intensity with the Helmholtz-Kirchhoff integral theorem[9] for the wave field amplitude to any point P_0 on the interior of a sphere S:

$$U(P_0) = \frac{ik}{4\pi}\int\int_S \left[\frac{\partial U}{\partial \eta}\frac{e^{ik|\mathbf{R}-\mathbf{r}|}}{ik|\mathbf{R}-\mathbf{r}|} - U\frac{\partial}{\partial \eta}\left(\frac{e^{ik|\mathbf{R}-\mathbf{r}|}}{ik|\mathbf{R}-\mathbf{r}|}\right)\right] d\sigma,$$

given the wave field on the surface. We have selected the center of the sphere S to lie at the photoemitting source so that the vector $\mathbf{R}$ for the converging spherical wave is parallel to $\hat{\mathbf{K}}$ for the hologram. Our image probe point $\mathbf{r}$ points from the photoemitter to P_0 and η is normal to the unit of surface area $d\sigma$ at $\mathbf{R}$. Under the Kirchhoff approximation we abruptly truncate the field at the edges of the hologram.

We are only interested in points P_0 which are atomic distances from the center of a macroscopic sphere. For these points the normal derivatives are simple and $|\mathbf{R}-\mathbf{r}| \approx R - \mathbf{r}\cdot\hat{\mathbf{R}}$. Using $\hat{\mathbf{K}} = \hat{\mathbf{R}}$ gives

$$U(\mathbf{r}) = \frac{1}{2\pi R^2}\int\int_S \chi(\hat{\mathbf{K}}) e^{-ik\mathbf{r}\cdot\hat{\mathbf{K}}} d\sigma.$$

Thus we should be able to find our image intensity at any point $\mathbf{r}$ by multiplying our hologram by a phase factor and integrating.

Guided by holographic optics we have arrived at an imaging integral which we can now show is in fact an inversion integral for photoelectron diffraction. Inserting Eq. (1) for $\chi(\hat{\mathbf{K}})$ in our integral and expanding the cosine as exponentials gives

$$U(\mathbf{r}) = \frac{1}{2\pi R^2}\sum_j \int\int_S [F(\theta_{r_jK}) e^{ikr_j} e^{ik(-\mathbf{r}_j-\mathbf{r})\cdot\hat{\mathbf{K}}} + F^*(\theta_{r_jK}) e^{-ikr_j} e^{ik(\mathbf{r}_j-\mathbf{r})\cdot\hat{\mathbf{K}}}] d\sigma_K.$$

For most values of $\mathbf{r}$, the exponential terms oscillate as $\hat{\mathbf{K}}$ explores the hologram and we get a small image intensity. When, however, $\mathbf{r} \approx \pm\mathbf{r}_j$ the exponential terms are always near 1 and a large image intensity can occur. Since $\mathbf{r}_j$ is the position of an atom, we anticipate an image of atomic structure from the holographic reconstruction. We shall also get twin images as in Gabor holography: For every $\mathbf{r}_j$ we shall see a twin atom at $-\mathbf{r}_j$.

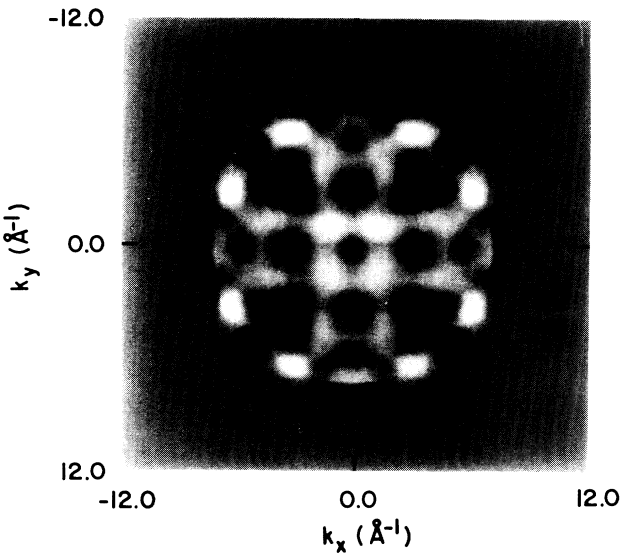

FIG. 1. Simulated photoelectron hologram for S(1s) photoemission from $c(2\times2)$S/Ni(001). The modulation in S(1s) intensity is shown as a function of $\hat{k}_x$ and $\hat{k}_y$, where the k values are zero in the center of the frame, and reach a value of 12.0 Å^{-1} at the edge. The photon electric vector is pointing to the right, 10° from the center. The simulation includes curved-wave corrections and multiple scattering.

The image intensity at $\mathbf{r} = \mathbf{r}_j$ will be an integral over the hologram angles of the generalized scattering factor F. As we approach integrating over a complete sphere, this integral will become proportional to the total cross section for elastic scattering; it will vary with the scattering atom and with the position of the sample with respect to the hologram.

In contrast to almost every other electron-scattering based probe for surfaces, the effect of multiple scattering of electrons on photoelectron holograms can be simply stated. Our image maxima occur near $\mathbf{r}_j$, the vector from the photoemitter to the last atom on any scattering path. All of the scattering events which exit through a given atom are imaged near that atom's atomic position. The size of the corresponding image maximum will depend in detail upon the sum of the scattering factors for these events.

The imaging integral looks very much like a Fourier integral, but it is not quite familiar since two hologram dimensions are transformed into three space dimensions. The precise analog is to the "angular spectrum of plane waves," the basis of the linear systems theory approach to optics.[12] This is clearer when we write the imaging surface integral in terms of K_x and K_y:

$$U(\mathbf{r}) = \frac{1}{2\pi R^2}\int_{-1}^{1}\int_{-1}^{1} \chi(\hat{\mathbf{K}}) \exp[ikz(1-\hat{K}_x^2-\hat{K}_y^2)^{1/2}] \exp(ikx\hat{K}_x + iky\hat{K}_y) d\hat{K}_x\, d\hat{K}_y. \quad (2)$$

This is certainly a double Fourier integral and we see that the z space dimension has the role of a parameter in the propagation phase shift for the image's third dimension. This remarkable result means that we can image surface structure by normalizing and phasing a two-dimensional photoelectron diffraction pattern and applying two-dimensional fast

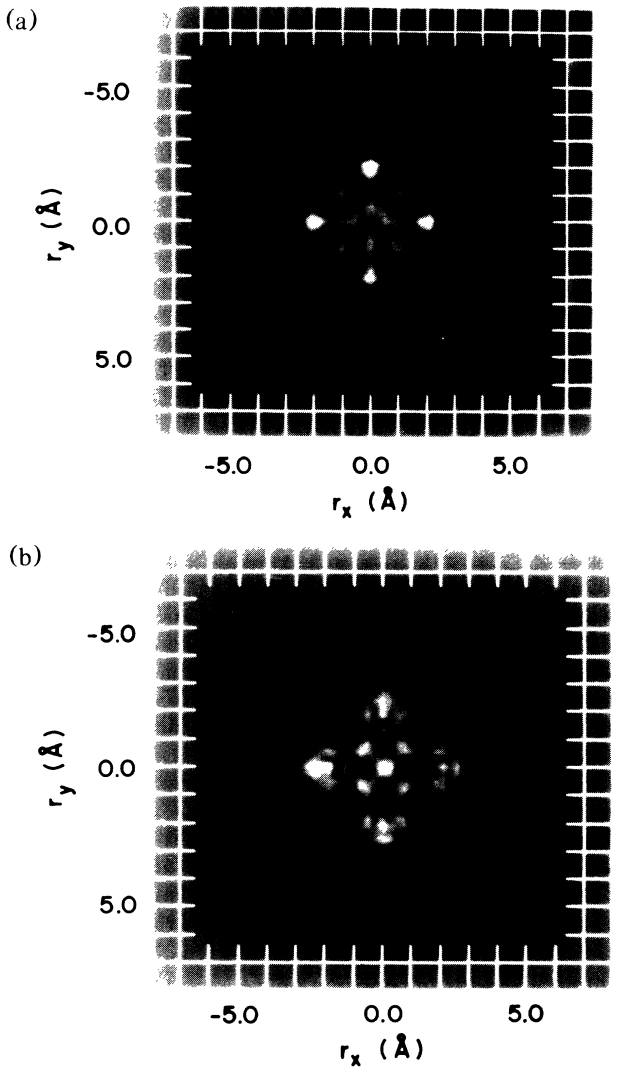

FIG. 2. Holographic reconstruction of Fig. 1. Each figure is a map of image intensity in a plane below the photoemitter and parallel to the hologram (and hence parallel to the surface plane) and spans 16.7 Å. The lines on the edges of the photographs are spaced by 1.0 Å. (a) A plane 1.29 Å below the emitter. (b) A plane 2.33 Å below the emitter.

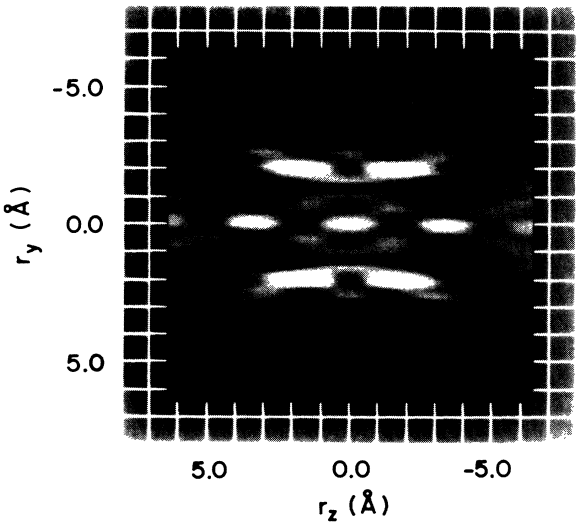

FIG. 3. A view in a plane perpendicular to the surface of the reconstructed image from the hologram in Fig. 1. The plane is a ⟨100⟩ plane containing the S photoemitter. The surface runs from top to bottom in the center of the picture. The image has inversion symmetry with all intensity to the left of center representing the conjugate image and that to the right of center being the real crystal image. The intensity maximum in the center of the image corresponds to the S atom visible through multiple scattering. Moving to the right, the two largest intensity features are the two Ni nearest neighbors in the ⟨100⟩ plane. Further to the right and vertically at the same height as the S atom appears the second nearest neighbor Ni directly below S and in the second Ni layer.

Fourier transforms!

To demonstrate the imaging capabilities of photoelectron holography, I have simulated the S(1s) photoelectron diffraction pattern for $c(2\times2)$S/Ni(001) using the multiple-scattering curved-wave theory of Ref. 10. Interference structure is visible in the hologram, Fig. 1, but it would not be possible to predict the structure from this picture. Applying the Fourier imaging integral with various values for z gives slices through the image parallel to the surface. The slice for $z=-1.29$ Å is shown in Fig. 2: The atomic positions of the four Ni nearest-neighbor atoms are clearly visible.

Figure 3 shows a slice perpendicular to the surface in a plane containing the S photoemitter. Two of the four Ni nearest-neighbor atoms are contained in this slice and their images are clearly visible. A third atom is also visible, it is the Ni atom in the second layer which is directly below the S photoemitter.

It is not possible to completely display the results from the Fourier inversion on paper: The image is three dimensional and any display will require some interpretation. Further investigation of the images might allow some perspective display to show more of the image than the slice technique used here.

Since the S adsorbate lies on top of the substrate, all of the twin images lie in an unphysical region of $+z$ values, a circumstance we cannot count on for arbitrary surfaces.

The resolution in the plane of the Ni atoms is close to the diffraction limit (0.5 Å) for the aperature (80° full opening angle) and energy (548 eV, $k=12$ Å^{-1}) used in this example. The vertical z-axis resolution is poorer, 2.3 Å, just adequate for structure work.

For quantitative work, we cannot rely directly on the peak maximum visible in the reconstructed image. The phase of the generalized scattering factor, F, will depend on $\hat{\mathbf{K}}$ and any linear dependence will shift the peak position. Accurate computation of this shift will require in-

cluding both curved-wave-front and multiple-scattering contributions,[10] but such calculations are greatly simplified because only paths which exit the crystal through one particular atom need be considered. Images reconstructed from simulations at electron energies other than the $k = 12$ Å^{-1} shown here have some spurious structure due to interference among multiple-scattering events centered near each atom. Unambigous images may require several holograms at different energies or sample orientations.

Photoelectron holography is a new way to use photoelectron diffraction to study the structure of solid surfaces. But it is a dramatically different way: Complete three-dimensional images of adsorption sites are now within reach. Photoelectron holography fulfills part of Gabor's vision of atomic resolution microscopy via holography;[1,8] it renews the promise of photoelectron diffraction as a surface structure method.

Is it a practical method? Only an experimental demonstration will be conclusive, but the measurements are certainly feasible (the simulation used here was based upon an existing two-dimensional electron analyzer), if a bit more sophisticated than most current photoelectron measurements. Considerable care will be required to obtain a properly normalized hologram with correctly assigned emission angles, but special care is not required in the crystal alignment: We need only specify relative electron emission angles. Accurate quantitative results will require correction for electron-scattering phase shifts.

In summary, no obstacle appears to block applications of photoelectron holography to the study of systems now feasible with photoelectron diffraction. The systems can be characterized as orientationally ordered systems with atomic species having unique photoemission lines, including subsurface adsorbates and buried interfaces. Less well-structured systems will give less well-structured images. Although photoelectrons have considerable experimental advantages, Auger electron holograms and electron energy loss holograms may also be feasible.

[1]A. Szöke, in *Short Wavelength Coherent Radiation: Generation and Applications,* edited by D. T. Attwood and J. Boker, AIP Conference Proceedings No. 147 (American Institute of Physics, New York, 1986).

[2]A. Liebsch, Phys. Rev. Lett. **32**, 1203 (1974).

[3]J. J. Barton, C. C. Bahr, S. W. Robey, Z. Hussain, E. Umbach, and D. A. Shirley, Phys. Rev. B **34**, 3807 (1986).

[4]K. C. Prince, E. Holup-Krappe, K. Horn, and D. P. Woodruff, Phys. Rev. B **32**, 4249 (1985).

[5]C. S. Fadley, Prog. Surf. Sci. **16**, 275 (1984).

[6]J. J. Barton, C. C. Bahr, Z. Hussain, S. W. Robey, J. G. Tobin, L. E. Klebanoff, and D. A. Shirley, Phys. Rev. Lett. **51**, 272 (1983).

[7]J. W. F. Egelhoff, Surf. Sci. **141**, L324 (1984).

[8]D. Gabor, Nature (London) **161**, 777 (1948).

[9]M. Born and E. Wolf, *Principles of Optics* (Pergamon, Oxford, 1980).

[10]J. J. Barton, S. W. Robey, and D. A. Shirley, Phys. Rev. B **34**, 778 (1986).

[11]J. J. Barton and D. A. Shirley, Phys. Rev. B **32**, 1892 (1985).

[12]J. W. Goodman, *Introduction to Fourier Optics* (McGraw-Hill, San Francisco, 1968).

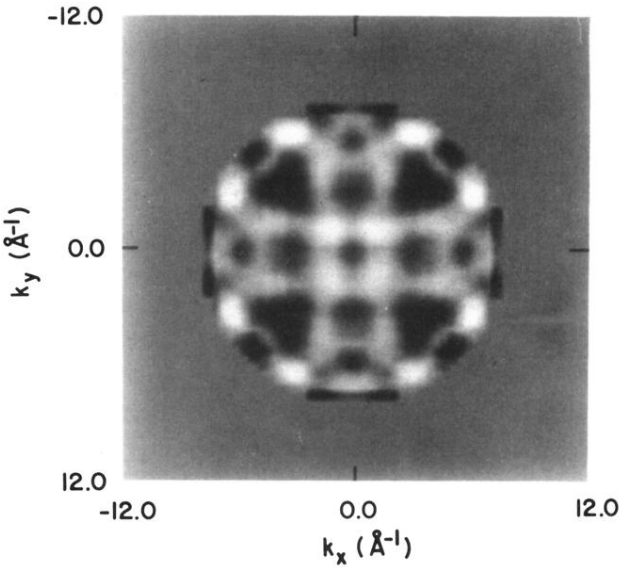

FIG. 1. Simulated photoelectron hologram for S(1s) photoemission from $c(2\times2)$S/Ni(001). The modulation in S(1s) intensity is shown as a function of $\hat{k}_x$ and $\hat{k}_y$, where the k values are zero in the center of the frame, and reach a value of 12.0 Å^{-1} at the edge. The photon electric vector is pointing to the right, 10° from the center. The simulation includes curved-wave corrections and multiple scattering.

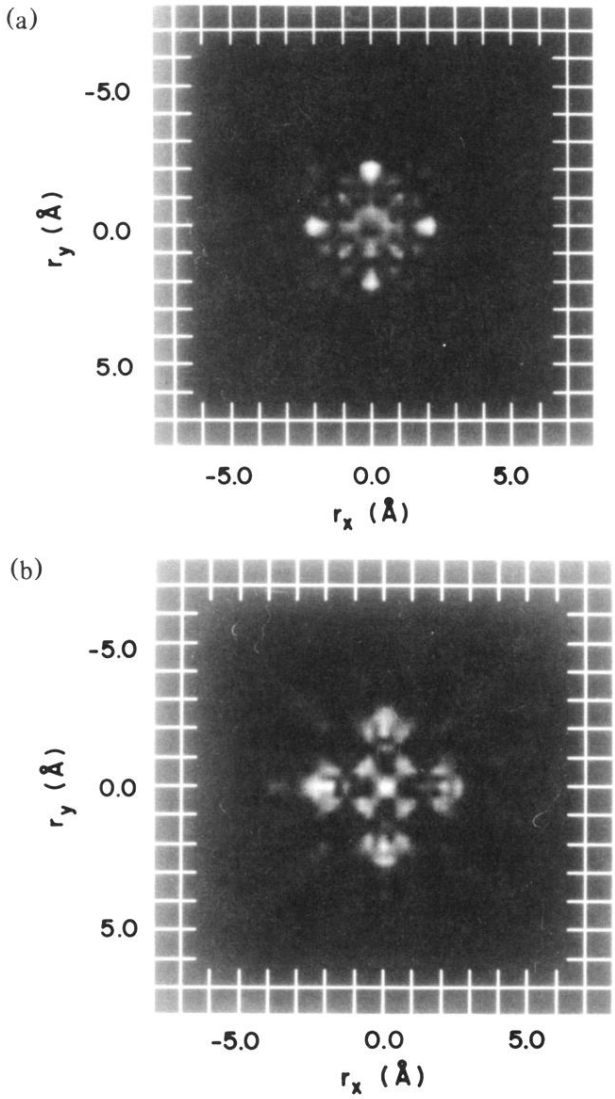

FIG. 2. Holographic reconstruction of Fig. 1. Each figure is a map of image intensity in a plane below the photoemitter and parallel to the hologram (and hence parallel to the surface plane) and spans 16.7 Å. The lines on the edges of the photographs are spaced by 1.0 Å. (a) A plane 1.29 Å below the emitter. (b) A plane 2.33 Å below the emitter.

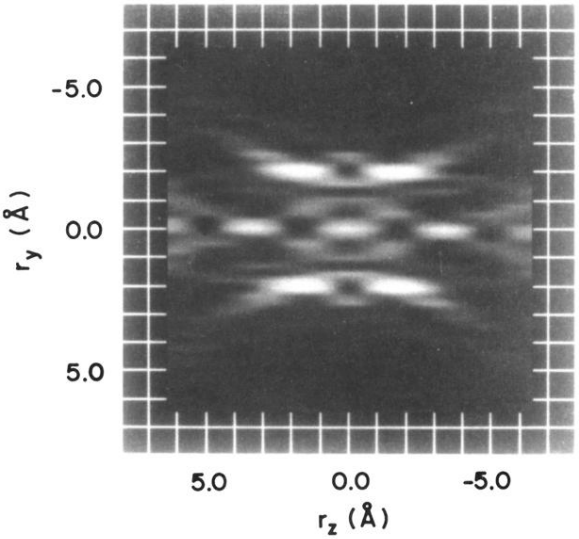

FIG. 3. A view in a plane perpendicular to the surface of the reconstructed image from the hologram in Fig. 1. The plane is a ⟨100⟩ plane containing the S photoemitter. The surface runs from top to bottom in the center of the picture. The image has inversion symmetry with all intensity to the left of center representing the conjugate image and that to the right of center being the real crystal image. The intensity maximum in the center of the image corresponds to the S atom visible through multiple scattering. Moving to the right, the two largest intensity features are the two Ni nearest neighbors in the ⟨100⟩ plane. Further to the right and vertically at the same height as the S atom appears the second nearest neighbor Ni directly below S and in the second Ni layer.